Suppression of Core Polarization in Halo Nuclei

T. T. S. Kuo,[1] F. Krmpotić,[2] and Y. Tzeng[3]
[1]*Department of Physics, SUNY-Stony Brook, Stony Brook, New York 11794*
[2]*Departamento de Fisica, Facultad de Ciencias Exactas, Universidad Nacional de La Plata, C. C. 67, 1900 La Plata, Argentina*
[3]*Institute of Physics, Academia Sinica, Nankang, Taipei, Taiwan*
(Received 18 June 1996; revised manuscript received 8 October 1996)

Halo nuclei are studied using a G-matrix interaction derived from the Paris and Bonn potentials and employing a two-frequency shell model approach. It is found that the core-polarization effect is dramatically suppressed in such nuclei. Consequently, the effective interaction for halo nucleons is almost entirely given by the bare G matrix alone, which presently can be evaluated with a high degree of accuracy. The experimental pairing energies between the two halo neutrons in ^{6}He and ^{11}Li nuclei are satisfactorily reproduced by our calculation. It is suggested that the fundamental nucleon-nucleon interaction can be probed in a clearer and more direct way in halo nuclei than in ordinary nuclei. [S0031-9007(97)02891-3]

PACS numbers: 21.30.Fe, 21.60.Cs

Radioactive-beam nuclear physics has been progressing rapidly, and there is much current interest in studying halo nuclei [1,2]. There were four articles about halo nuclei in a recent issue of Physical Review C: Nazarewicz *et al.* [3] dealt with the halo nuclei around the nucleus ^{48}Ni, Hamamoto *et al.* [4] carried out a systematic investigation of the single particle and collective degrees of freedom in the drip-line nuclei, and an experimental study of heavy halo nuclei around $N = 82$ was also presented [5]. It is remarkable that nuclei as exotic as ^{48}Ni, i.e., the mirror image of the double closed-shell nucleus ^{48}Ca, are now being studied.

The halo nuclei (or drip-line nuclei) may well play a central role in our understanding of the nuclear binding. Their typical structure is that of a tightly bound inner core with a few outer nucleons that are loosely attached to the core. Although these exotic nuclei are bound, their binary subsystems are not. For instance, the halo nucleus ^{6}He (^{11}Li) is presumably made of a ^{4}He (^{9}Li) core surrounded by a two-neutron halo. As a whole ^{6}He (^{11}Li) is bound, but its binary subsystems, i.e., ^{5}He (^{10}Li) and the *dineutron* are unbound. The pairing force between the valence nucleons is thus essential for the stability of the halo nuclei, and it is important to calculate it as accurately as we can.

So far, the halo nuclei have been calculated using empirical effective interactions, tuned to stable nuclei. The inherent density dependence of Skyrme-type forces [3,4] provides a reasonable means of extrapolating to the lower density regimes characteristic of nuclei far from stability. Yet, quite recently Kuo *et al.* [6] have suggested studying the drip-line nuclei from the first principles, i.e., from the elementary nucleon-nucleon (NN) force, such as the Paris [7] and Bonn [8] interactions. Halo nucleons are separated rather far from the other nucleons in the "core nucleus," and the interaction among them should be derivable from the free NN interaction with small medium corrections.

The effective interaction ($V_{\rm eff}$), among the nucleons in the nuclear medium, can be derived from the free NN interaction, using a G-matrix folded-diagram approach [9,10]. The major difficulty in such a microscopic effective interaction theory is the treatment of the core polarization effect (CPE), and in particular of that due to the higher-order diagrams. In ordinary nuclei, the valence nucleons are close to the nuclear core, an example being the two sd-shell neutrons of ^{18}O residing adjacently to the ^{16}O core. Consequently, there is a strong valence-core coupling and therefore a large CPE. In such a situation it is a formidable task to figure out which irreducible linked-diagrams diagrams should be embodied in the vertex function $\hat{Q}$ (often referred to as the $\hat{Q}$ box) on which the calculation of $V_{\rm eff}$ is based [9]. The two leading terms in the $\hat{Q}$ box are the well-known first-order G-matrix diagram and the second-order core polarization diagrams, denoted, respectively, by G and G_{3p1h} [11]. Hjorth-Jensen *et al.* [12] have investigated the third-order $\hat{Q}$-box diagrams for the sd shell. They concluded that, after folding, the net effect on $V_{\rm eff}$ was a change of about 10%–15%, as compared with the case when only the first- and second-order ones were considered. Higher and higher-order core polarization diagrams rapidly become prohibitively more difficult to deal with. Thus in practice one can only include some low-order diagrams for the calculation of the $\hat{Q}$ box. Besides, when there are disagreements between theory and experiment, one is not sure if they are due to the NN interaction or to the approximation adopted in solving the many-body problems (such as the neglecting of the higher-order core polarization diagrams).

The framework is different in halo nuclei and may be more promising; a schematic comparison between normal and halo nuclei is given in Fig. 1. Because the halo nucleons are located quite far away from the core, a relatively weak CPE is expected in halo nuclei. Thus, $V_{\rm eff}$ should be both (i) governed predominantly by the free NN interaction, and (ii) given in essence by the bare G matrix, which presently can be calculated to a high degree of accuracy. Hence the halo nuclei, besides having

 0031-9007/97/78(14)/2708(4)$10.00

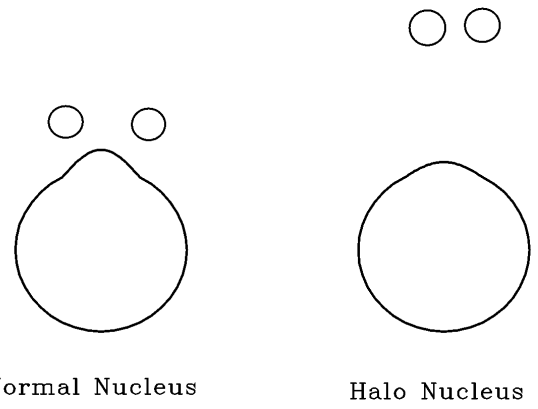

FIG. 1. Comparison of core polarization in ordinary and halo nuclei.

excitingly interesting and exotic properties, may furnish as well a much better testing ground for the fundamental *NN* interactions than ordinary nuclei. Motivated by the above scenario, we present in this Letter a G-matrix folded-diagram [9,10] derivation of the $V_{\rm eff}$ for halo nucleons in ^{6}He and ^{11}Li, starting from the Paris and Bonn *NN* potentials and with a special attention to the CPE in halo nuclei. The main steps in such a derivation are as follows.

(1) Choice of the model space P.—An important criterion for selecting the model space P is that its overlap, with the physical states under consideration, should be as large as possible. For instance, the ^{4}He, i.e., the ^{6}He core, should remain essentially as an ordinary α particle, with little perturbation from the distant halo nucleons. For the P space we shall use a closed $(0s_{1/2})^4$ core (α particle) with the valence (halo) nucleons confined in the $0p$ shell. Yet the halo nucleons have a much larger r.m.s. radius than the core, and therefore an oscillator constant $\hbar\omega$ considerably smaller than that given by the empirical formula $\hbar\omega = 45A^{-1/3} - 25A^{-2/3}$ MeV (valid for ordinary nuclei). It would not then be feasible to reproduce both radii, using shell model wave functions with a common $\hbar\omega$. One may get past this difficulty by including several major shells in the one-frequency shell model (OFSM) calculation. But this would be very tedious. A convenient and physically appealing solution to this problem is to employ a two-frequency shell model (TFSM) for the description of halo nuclei, as suggested in Ref. [6]. Within the TFSM one uses oscillator wave functions with $\hbar\omega_{\rm in}$ and $\hbar\omega_{\rm out}$ for the core (inner) and the halo (outer) orbits, respectively. The notations $b_{\rm in}$ and $b_{\rm out}$ also will be used from now on, with $b^2 \equiv \hbar/m\omega$. In the present work $b_{\rm in}$ is fixed at 1.45 fm, while our $b_{\rm out}$ value is chosen under the constraint that it satisfactorily reproduces the experimental r.m.s. radius of the halo nucleus under consideration. To assure the orthonormality, we have actually used $b_{\rm in}$ for all the $\ell = 0$ waves $(0s_{1/2}, 1s_{1/2}, \ldots)$ and $b_{\rm out}$ for waves with other ℓ values.

(2) Evaluation of the model-space G matrix.—For ordinary nuclei, the G matrix can be calculated rather accurately with the method developed in Refs. [13,14]. We extend below this method to the halo nucleons in the context of the TFSM [6]. For a general model-space P, we define the corresponding Brueckner G matrix by the integral equation [14,15]

$$G(\omega) = V + VQ_2 \frac{1}{\omega - Q_2 T Q_2} Q_2 G(\omega),$$

where ω is an energy variable, Q_2 is a two-body Pauli exclusion operator, and T is the two-nucleon kinetic energy. Note that our G matrix has orthogonalized plane-wave intermediate states. The exact solution of this G matrix is $G = G_F + \Delta G$ [13,14], where G_F is the *free* G matrix, and ΔG is the Pauli correction term

$$\Delta G(\omega) = -G_F(\omega)\frac{1}{e}P_2 \frac{1}{P_2[\frac{1}{e} + \frac{1}{e}G_F(\omega)\frac{1}{e}]P_2} \times P_2 \frac{1}{e} G_F(\omega),$$

with $e \equiv \omega - T$. The projection operator P_2, defined as $(1 - Q_2)$, will be discussed later. The basic ingredient for calculating the above G matrix is the matrix elements of G_F within the P_2 space. This space contains all the two-particle states that must be excluded from the intermediate states in G-matrix calculations. For ordinary nuclei, where the OFSM is used, the states excluded by the Pauli operator and those contained within the model space have a common length parameter b. For halo nuclei, where we use the TFSM, the situation is more complicated, as the wave functions for the excluded states and those within the model space have in general different length parameters $b_{\rm in}$ and $b_{\rm out}$. Hence to calculate ΔG, we need the matrix elements of G_F in a $b_{\rm in} - b_{\rm out}$ mixed representation. This poses a technical difficulty because the transformations, from the c.m. coordinates to the laboratory coordinates for two-particle states with different oscillator lengths, are not as easy to perform as for one common oscillator length. We have adopted an expansion procedure to surmount this difficulty. Namely, we expand the oscillator wave functions with $b_{\rm in}$ in terms of those with $b_{\rm out}$, or vice versa. When $b_{\rm in}$ and $b_{\rm out}$ are not too different from each other, this procedure is relatively effortless to carry out. Usually a high accuracy can be attained by including about eight terms in the expansion. Still, the calculation of the two-frequency G matrix is significantly more complicated than the ordinary one-frequency one. Another difficulty, in deriving the G matrix for halo nuclei, is the treatment of its Pauli exclusion operator. As the halo nucleons are rather far from the core nucleons, the effect of Pauli blocking is expected to be small. But, to get a reliable result for a small effect, a very accurate procedure has to be employed. We write the projection operator Q_2 as

$$Q_2 = \sum_{\rm all\ } Q(ab)\,|ab\rangle\langle ab|,$$

where $Q(ab) = 0$, if $b \le n_1$, $a \le n_3$, or $b \le n_2$, $a \le n_2$, or $b \le n_3$, $a \le n_1$, and $Q(ab) = 1$ otherwise. The

boundary of $Q(ab)$ is specified by the orbital numbers (n_1, n_2, n_3). We denote the shell model orbits by numerals, starting from the bottom of the oscillator well: 1 for orbit $0s_{1/2}$, 2 for $0p_{3/2}, \ldots,$ 7 for $0f_{7/2}$, and so on. n_1 and n_2 stand for the highest orbits of the closed core (Fermi sea) and of the chosen model space, respectively. For example, we consider ^{4}He as a closed core and all six orbits in the sp and sd shells are included in the model space. Then $n_1 = 1$ and $n_2 = 6$. As for the G-matrix intermediate states we consider only particle states (i.e., states above the Fermi sea), n_3 in principle should be ∞ [14]. Still, in practice this is not feasible, and n_3 has to be determined by an empirical procedure. Namely, we perform calculations with increasing values for n_3 until numerical results become stable. In Table I, we display some representative results of our two-frequency G matrix for the $\{0s0p\}$ model space, with $b_{\text{in}} = 1.45$ fm and $b_{\text{out}} = 2.0$ fm. The only approximation here is the finite n_3 truncation. A satisfactory n_3 convergence is attained for $n_3 = 21$, and this value is used here. It is worth noting that, although the halo nucleons are widely separated from the closed core, the Pauli correction term $\Delta G(= G - G_F)$ is still quite significant.

(3) Calculation of the irreducible diagrams for the vertex function $\hat{Q}$.—The effective interaction is given as a $\hat{Q}$-box folded-diagram series [9,10], of the form

$$V_{\text{eff}} = \hat{Q} - \hat{Q}' \int \hat{Q} + \hat{Q}' \int \hat{Q} \int \hat{Q} - \hat{Q}' \int \hat{Q} \int \hat{Q} \int \hat{Q} \cdots ,$$

where the integral sign represents a generalized folding operation. $\hat{Q}'$ box and $\hat{Q}$ box are both irreducible vertex functions, and they are the same except that the former begins with second-order diagrams in the NN interaction. To get V_{eff} one has to calculate the irreducible $\hat{Q}$-box diagrams and their energy derivatives, in terms of the model-space-dependent G matrix. In the present work, we include in the $\hat{Q}$-box valence-linked diagrams first- and second-order in the G matrix [11]. We point out that, although the G matrix is manifestly energy (ω) dependent (see Table I), V_{eff} *is not* because of the inclusion of the folded diagrams [9].

TABLE I. Dependence of the two-frequency G matrix on the choice of n_3. Listed are the matrix element $\langle (0p_{3/2})^2; TJ|G(\omega)|(0p_{3/2})^2; TJ\rangle$ (in MeV), calculated for the Paris potential and three different values of ω (in MeV), with $TJ = 01$ (upper panel) and with $TJ = 10$ (lower panel). We have used $b_{\text{in}} = 1.45$ and $b_{\text{out}} = 2.0$ fm for the length parameters, and $n_1 = 1$ and $n_2 = 6$ for the exclusion operator. The first row in each group (F) denotes the free G matrix.

n_3	$\omega = -5$	$\omega = -10$	$\omega = -20$
F	−6.896	−4.530	−3.155
6	−2.218	−2.115	−1.885
15	−2.217	−2.114	−1.882
21	−2.217	−2.114	−1.882
F	−4.422	−3.933	−3.480
6	−2.768	−2.748	−2.701
15	−2.761	−2.744	−2.698
21	−2.761	−2.744	−2.698

Diagonal matrix elements of G, G_{3p1h}, and V_{eff}, for the states $|(p_{3/2})^2; T = 1, J = 0\rangle$ and $|(p_{1/2})^2; T = 1, J = 0\rangle$, are shown in Fig. 2 as a function of b_{out}, for both the Paris and Bonn A potentials. As we increase b_{out}, we are augmenting the average distance between the halo nucleons and the core and so reducing the coupling between them. For sufficiently large b_{out}, the total CPE must be small and it should be sufficiently accurately given by the second-order (lowest order) core polarization diagram alone. In fact, as b_{out} increases, the core polarization diagrams G_{3p1h} approach rapidly and monotonically to zero and become negligibly small at $b_{\text{out}} \cong 2.25$ fm. In our TFSM approach, we have assumed a fixed ^{4}He core, always described by $b_{\text{in}} = 1.45$ fm. Therefore the energy denominator for the diagram G_{3p1h} is fixed by the corresponding core and does not change with b_{out}. This means that the suppression of G_{3p1h} is entirely due to the weakening of the core-valence particle interaction. The behavior of the bare G matrix and V_{eff} shown in Fig. 2 are also of interest. First, they are quite similar to each other. Second, while for the $p_{3/2}$ case, they become weaker as b_{out} increases, in the $p_{1/2}$ case they become stronger as b_{out} increases. Third, at large b_{out} the results given by the Paris and Bonn A potentials are practically identical. This is because their long-range parts do not differ much from each other.

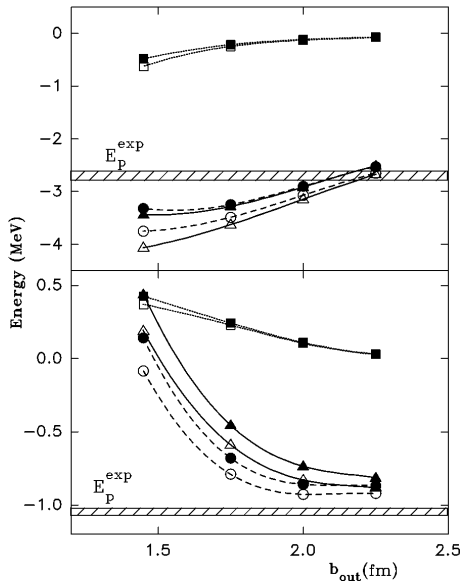

FIG. 2. Diagonal matrix elements of G_{3p1h} (dotted lines), G (dashed lines), and V_{eff} (full lines) for the states $|(p_{3/2})^2; T = 1, J = 0\rangle$ (upper panel) and $|(p_{1/2})^2; T = 1, J = 0\rangle$ (lower panel) as a function of b_{out}; calculations done with Paris and Bonn A potentials are shown by open and solid symbols, respectively. The G-matrix curves are for $\omega = -5$ MeV and Pauli exclusion operator with $(n_1, n_2, n_3) = (1, 3, 21)$.

To assess to which extent the nuclear model formulated above is reliable it is necessary to compare our results with experiments.

^{6}He nucleus.—The measured r.m.s. radius is $R^{\rm exp}(^6{\rm He}) = 2.57 \pm 0.1$ fm [16], while the experimental valence or pairing interaction energy between the halo nucleons is gathered from the odd-even mass difference [17]

$$E_p^{\rm exp}(^6{\rm He}) = -[\mathcal{B}(^6{\rm He}) + \mathcal{B}(^4{\rm He}) - 2\mathcal{B}(^5{\rm He})] = -2.77\ {\rm MeV}\,.$$

The corresponding theoretical values are obtained by diagonalizing $V_{\rm eff}$ in a $\{p_{3/2}, p_{1/2}\}$ model space with the $(T = 1, J = 0)$ coupling. We found that both measured quantities are well reproduced by the calculation for $b_{\rm out} = 2.25$ fm. Our calculated results are $R^{\rm th}(^6{\rm He}) = 2.51$ fm, and $E_p^{\rm th}(^6{\rm He}) = -2.97$ MeV (for the Paris potential). As the CPE is strongly suppressed for such a $b_{\rm out}$ value, this result almost entirely comes from the bare G matrix. Moreover, the ground-state wave function is almost a pure $|(p_{3/2})^2; T = 1, J = 0\rangle$ state with very little $(p_{1/2})^2$ admixture. Thus our $E_p^{\rm th}$ is mainly given by the diagonal G-matrix element as indicated in Fig. 2.

^{11}Li nucleus.—Here $R^{\rm exp}(^{11}{\rm Li}) = 3.1 \pm 0.1$ fm [16], and from the masses of ^{11}Li, ^{10}Li, and ^{9}Li [17] one gets $E_p^{\rm exp}(^{11}{\rm Li}) = -1.14$ MeV. As we have used the $\{p_{3/2}, p_{1/2}\}$ model space, our wave function has only one component (neutron orbits closed). Then the diagonal $(p_{1/2})^2(T = 1, J = 0)$ matrix element of $V_{\rm eff}$ is directly comparable to the pairing energy. Also in this case the measured rms radius is well accounted for by the calculation with $b_{\rm out} = 2.25$ fm, but the theoretical pairing energy turns out to be somewhat too small. For the Paris potential we get $R^{\rm th}(^{11}{\rm Li}) = 3.03$ fm and $E_p^{\rm th}(^{11}{\rm Li}) = -0.81$ MeV. The difference between $E_p^{\rm exp}$ and $E_p^{\rm th}$ could be pointing out that some physics is still missing in our description of the valence ^{11}Li neutrons. It is very likely that they should not be entirely confined to the p shell, but a larger space, such as $\{0p_{1/2}0d1s\}$, is probably needed.

We have also calculated the valence interaction energy for ^{6}Li using a similar folded-diagram procedure in the $\{p_{3/2}, p_{1/2}\}$ space. From the empirical masses of ^{6}Li, ^{5}Li, ^{5}He, and ^{4}He [17], we obtain $E_v^{\rm exp} = -6.56$ MeV. (This number was incorrectly given as -3.55 MeV MeV in Ref. [6].) Our result is $E_v^{\rm th} = -6.64$ MeV for the Paris potential, if we use $b_{\rm in} = 1.45$ fm fm and $b_{\rm out} = 1.75$ fm. It is of interest to stress that ^{6}Li is *not* a halo nucleus, according to our calculation, in the sense that there is no need to employ a very large $b_{\rm out}$ for its valence nucleons.

In summary, we have derived the effective interaction for the valence nucleons in halo nuclei, starting from realistic *NN* interactions. Our preliminary results are encouraging. We have employed a two-frequency shell model approach, to give a good spatial description for both the core nucleons and the halo nucleons. With $b_{\rm in}$ and $b_{\rm out}$ fixed, respectively, at 1.45 and 2.25 fm, we have obtained good agreements with experiments for both the pairing energies of the ^{6}He and ^{11}Li halo neutrons and the r.m.s. radii of these nuclei. Also, for an outer length parameter compatible with the large empirical r.m.s. radii of halo nuclei, a dramatic suppression of the core polarization effect is observed; therefore, *the effective interaction between the halo nucleons is predominantly given by the bare G matrix alone,* in accord with our expectations. The Pauli blocking effect on the G matrix has been found to be very important, and it can be calculated quite accurately as we have demonstrated. Thus it appears that one can derive the effective interaction for halo nuclei much more accurately than for ordinary nuclei. We enthusiastically believe that the halo nuclei, which have already greatly enhanced our knowledge about nuclei, may in addition provide a more accurate testing ground for the fundamental *NN* interaction than the ordinary nuclei.

This work is supported in part by the U.S. DOE Grant No. DE-FG02-88ER40388, by the NSF Grant and by the Fundación Antorchas (Argentina). One of us (T. T. S. K.) is grateful for the warm hospitality extended to him while visiting the Universidad Nacional de La Plata.

[1] S. M. Austin and G. F. Bertsch, Sci. Am. **272**, 62 (1995).
[2] J. S. Al-Khalili, Phys. Rev. Lett. **76**, 3903 (1996).
[3] W. Nazarewicz *et al.*, Phys. Rev. C **53**, 740 (1996).
[4] I. Hamamoto, H. Sagawa, and X. L. Zhang, Phys. Rev. C **53**, 765 (1996); I. Hamamoto and H. Sagawa, Phys. Rev. C **53**, 1492 (1996).
[5] R. D. Page *et al.*, Phys. Rev. C **53**, 660 (1996).
[6] T. T. S. Kuo, H. Muether, and X. Azimi-Nilli, Nucl. Phys. **A606**, 16 (1996).
[7] M. Lacombe *et al.*, Phys. Rev. C **21**, 861 (1980).
[8] R. Machleidt, Adv. Nucl. Phys. **19**, 189 (1989).
[9] T. T. S. Kuo and E. Osnes, *Lecture Notes in Physics* (Springer-Verlag, Berlin, 1990), Vol. **364**, p. 1.
[10] T. T. S. Kuo, E. Krmpotić, K. Suzuki, and R. Okamoto, Nucl. Phys. **A582**, 205 (1995).
[11] J. Shurpin, T. T. S. Kuo, and D. Strottman, Nucl. Phys. **A408**, 310 (1983).
[12] M. Hjorth-Jensen, T. T. S. Kuo, and E. Osnes, Phys. Rep. **261**, 126 (1995).
[13] S. F. Tsai and T. T. S. Kuo, Phys. Lett. **39B**, 427 (1972).
[14] E. M. Krenciglowa, C. L. Kung, T. T. S. Kuo, and E. Osnes, Ann. Phys. (N.Y.) **101**, 154 (1976).
[15] H. Müther and P. Sauer, in *Computational Nuclear Physics*, edited by K. Langanke, J. A. Maruhn, and S. Koonin (Springer-Verlag, Berlin, 1992), Vol. **2**, p. 30.
[16] M. V. Zhukov *et al.*, Phys. Rep. **231**, 151 (1993), and references therein.
[17] *Nuclear Wallet Cards*, edited by J. K. Tuli (National Nuclear Data Center, Brookhaven National Laboratory, Upton, New York, 1995).